On the Mechanism of Rapid Plasma Membrane and Chloroplast Envelope Expansion in *Dunaliella salina* Exposed to Hypoosmotic Shock

Manabu Maeda and Guy A. Thompson, Jr.

Department of Botany, University of Texas, Austin, Texas 78713

Abstract. *Dunaliella salina* cells rapidly diluted from their normal 1.71 M NaCl-containing growth medium into medium containing 0.86 M NaCl swelled within 2–4 min to an average volume 1.76× larger and a surface area 1.53× larger than found in control cells. Morphometric analysis of thin section electron micrographs revealed that certain organelles, including the chloroplast, nucleus, and some types of vacuoles, also expanded in surface area as much or more than did the entire cell. It is likely that glycerol, the most important osmotically active intracellular solute, was present in high concentration within these organelles as well as in the cytoplasm itself.

Thin section and freeze-fracture electron microscopy were utilized to trace the origin of membrane material whose addition permitted the large increase in plasma membrane surface area and the equally large growth of the chloroplast outer envelope. The findings indicated that the plasma membrane's expansion resulted from its selective fusion with numerous small (≤0.25 μm diam) vesicles prevalent throughout the cytoplasm. In contrast, new membrane added to the chloroplast outer envelope was drawn from an entirely different source, namely, elements of the endoplasmic reticulum.

ALGAE of the genus *Dunaliella* have been the subject of intense study because of their ability to survive a wide range of salinity (3). *Dunaliella* species can readily adapt to growth in waters ranging from 0.5 to 5 M NaCl. The osmotic balance is maintained by matching the external inorganic ions with internal glycerol (1, 3). In nature the cells sometimes have occasion to cope with rapid dilution of their surrounding medium, e.g., in cases where the shallow ponds they inhabit are flooded with rainwater. Although osmoregulation by enzymatically altering the absolute levels of cytoplasmic glycerol is remarkably fast (11), temporary osmotic inbalances must invariably occur. The cells respond to rapid dilution in a different way, namely by absorbing water and expanding, thereby diluting their internal glycerol to match the reduced extracellular salt level.

This latter response is possible because *Dunaliella*, which resembles other plant cells in most aspects of its general structure (3, 11), lacks a rigid cell wall and thus has a relatively unrestricted capacity for volume expansion. Almost instantaneous increases in cell surface area of as much as 400% (6) have been observed after sudden dilution. The source of the additional membrane material needed for plasmalemma expansion is not known. In this communication we describe experiments that clarify the mechanism permitting a large scale surface area expansion of the plasmalemma and other membranes.

Materials and Methods

Culture Conditions

Axenic cultures of *Dunaliella salina* (UTEX 1644) were grown in synthetic medium as described by Lynch and Thompson (13). Cultures were grown to the mid-logarithmic stage (0.5–1.0 × 10^6 cells/ml) at 30°C under continuous light (500 μE μm^{-2} s^{-1}) in 1-liter Erlenmeyer flasks containing 500 ml medium bubbled with 0.5% CO_2-enriched air.

Light Microscopy

Cell shape and length alterations due to hypoosmotic stress were observed by light microscopy beginning within 10 s after dilution with NaCl-free synthetic medium. The experiments were carried out three times using logarithmic phase cells. More than 10 micrographs (× 400) were prepared for the measurement of the half diameters of the major axis and the minor axis of control and diluted cells.

Cell Volume and Surface Area of Plasma Membrane

Cell volumes were calculated assuming control cells to be prolate ellipsoids ($v = 4/3\pi ab^2$, where $a \geq b$) and diluted cells spheres ($v = 4/3\pi r^3$). Surface areas of control cells were determinated by using the formula $s = 2\pi(b^2 + a^2/\xi \text{ arcsinh } b\xi/a$, where $\xi^2 = 1 - (b/a)^2$ and $a > b$ (20) or, for the spherical swollen cells, $s = 4\pi r^2$, where $r = a = b$.

Electron Microscopy

Most samples to be used for freeze-fracture studies were fixed for 2–3 h at 30°C under illumination with 2–2.5% glutaraldehyde buffered with the synthetic medium for *Dunaliella salina* as described by Lynch and Thompson (13).

After washing three times with synthetic medium, fixed samples were

Table I. Changes in Cell Volume and Cell Surface Area Caused by Hypoosmotic Shock

	Control					Diluted culture*				
	n	$\bar{a}$	$\bar{b}$	Volume	Surface area	*n*	$\bar{a}$	$\bar{b}$	Volume	Surface area
Exp. 1	20	5.89 ± 0.95	4.83 ± 0.41	586.4 ± 163.7	321.7 ± 56.9	20	6.55 ± 0.84	6.48 ± 0.79	1,202.0 ± 440.6	536.9 ± 131.2
Exp. 2	20	5.88 ± 0.75	5.06 ± 0.53	645.9 ± 191.1	346.3 ± 69.1	20	6.20 ± 0.73	6.08 ± 0.71	996.7 ± 402.5‡	478.8 ± 120.5
Exp. 3	17	6.37 ± 0.52	4.47 ± 0.48	540.0 ± 129.4	299.5 ± 50.0	13	6.15 ± 0.33	5.96 ± 0.42	915.5 ± 186.4	464.2 ± 76.7
Mean		6.05 μm	4.79 μm	590.8 μm^3/cell	322.5 μm^2/cell		6.30 μm	6.17 μm	1,038.1 μm^3/cell	493.3 μm^2/cell
Increase									× 1.76	× 1.53

Values of *a*, *b*, volume, and surface area are means ± SD. Except where indicated, differences between diluted and control values are statistically significant at the 0.001 level. *n*, cell number counted; $\bar{a}$, average half diameter of major axis; $\bar{b}$, average half diameter of minor axis ($a \geq b$).

* Cells were photographed 3 ± 1 min after medium was diluted from 1.71–0.86 M NaCl.

‡Significantly different from controls at the 0.005 level.

transferred to increasing concentrations of glycerol, terminating with 30% glycerol buffered with the synthetic medium.

The cells were pelleted in a clinical centrifuge (1,500 *g* for 5 min) and samples were frozen in liquid Freon before being fractured in a Balzers BF 400 device (Balzers, Hudson, NH). Replication was performed with platinum–carbon, and the replicas were coated with carbon. After residual tissue was digested from the replicas with Clorox, they were given three rinses in water before collection on 300–400-mesh grids.

In some cases control cells or cells freshly diluted to 0.86 M NaCl were pelleted in a clinical centrifuge (1,500 *g* for 3 min) and directly frozen in liquid Freon without fixation and added cryoprotectant. These cells were then processed for freeze fracture electron microscopy as described above for the glutaraldehyde-fixed cells.

The electron microscopic observations were performed with a Hitachi-11E electron microscope operating at 50 kV (Hitachi Ltd., Allendale, PA). Intramembranous particles (IMP)[1] were counted in 10–46 randomly selected areas (0.2 × 0.2 μm^2) of several different micrographs enlarged to × 48,000 or × 60,000, and particle density was expressed as particles/μm^2.

Samples to be used for preparing thin sections were fixed in 2–2.5% glutaraldehyde by the same method described above. After being rinsed three times in synthetic medium, samples were postfixed in 1% (wt/vol) OsO_4 for 1 h, transferred to 25% acetone for 30 min, and then to increasing concentrations of acetone, terminating with 100% acetone for dehydration. Finally, they were embedded in Spurr's low viscosity medium (16). Sections cut on a MT-1 microtome were collected on 300–400-mesh grids, stained in uranyl acetate (3 min), and then in lead citrate (3 min). Micrographs were made by using a Hitachi-11E electron microscope at an accelerating voltage of 50 kV.

Morphometric Analysis (Stereology)

Many thin section electron micrographs were utilized for morphometric analysis following techniques described by Weibel (20). Regular lattice grid points (distance between points [*d*] = 5 mm and 15 mm) were counted on the micrographs (× 4,600 or × 16,000, respectively) of control and diluted cells for obtaining actual volumes of vacuoles, chloroplast, nuclei, mitchondria, and Golgi bodies. For morphometry, vesicles were categorized as being small (≤ 0.25-μm diam), usually appearing empty but occasionally with even smaller vesicles within. These structures were widely distributed within the cell and were particularly noticeable in the cytoplasm just below the plasma membrane (PM). Vacuoles were structures having a diameter larger (often much larger) than 0.25-μm, sometimes containing smaller vesicles and other membranous material within. The vacuoles were mainly localized in the cytoplasm anterior to the chloroplast.

Estimation of actual surface area of chloroplasts, mitochondria, nuclei, Golgi, vesicles, and vacuoles was carried out by counting intersection numbers (I_t) with a lattice grid (d = 25 mm) on a minimum of 19 separate micrographs (× 48,000) of control and diluted cells. The surface area of small vesicles and other membranous structures seen within vesicles and vacuoles was estimated by the same method on × 48,000 micrographs using a smaller lattice grid (d = 5 mm).

Estimation of endoplasmic reticulum (ER) surface area was achieved by counting their intersections with a curvilinear grid (Merz pattern, d = 30 mm) on the micrographs (× 48,000) of control and diluted cells. The average surface area of specific organelles per μm^3 of cell volume (S_v) was calculated from the formula $S_v = 2I_t/k \cdot d \cdot P_t$, where k is 2 (lattice grid) or 1.57 (Merz pattern), d is d corrected to actual magnification, P_t is total number of grid points within the internal cell area, and I_t is the total intersections with the lattice grid. Then the total surface area per cell (S_t) was calculated from S_v and the actual cell volume (see Table I).

[1] *Abbreviations used in this paper:* ER, endoplasmic reticulum; IMP, intramembranous particles; PM, plasma membrane.

Results

General Effects of Osmotic Stress on Cell Size

For the present studies *D. salina* was routinely grown in a medium containing 1.71 M NaCl. Fig. 1 shows light micrographs of (*a*) control cells and (*b*) cells photographed 3 ± 1 min after being diluted to 0.86 M NaCl by a rapid (5 s) addition of NaCl-free synthetic medium or distilled water. Dilution caused an almost immediate expansion of the cells from their typical oval shape to a sphere (Fig. 1, *a* and *b*).

An examination of thin sections cut through the central regions of numerous cells confirmed the change in shape and size of the diluted cells that was first observed by light microscopy of living cells and showed that internal organelles, particularly vacuoles and the single large chloroplast, also swelled after dilution (Fig. 1, *c* and *d*).

After a period of ~3 min, the cells sustained no further expansion and gradually decreased in size over a period of 16 h until they regained their original shape and size. Based on surface area measurements made from light micrographs (Table I), the average cell's volume and surface area were calculated to increase during the initial swelling by 1.76× and 1.53×, respectively. Measurements made on thin section micrographs of these cells revealed that several of the intracellular organelles also increased in volume (Table II) and surface area (Table III) after dilution. Although greater expansions have been observed by more drastic dilutions, we confine our discussions here to the 1.71–0.86 M NaCl dilution because it can be achieved very rapidly with a high rate of cell survival.

Effects of Hypoosmotic Stress on PM Structure

Freeze-fracture replicas made of cells immediately after dilution (Fig. 2) and 3 min after dilution (Fig. 3, *a* and *b*) revealed significant changes in the PM appearance. Fig. 2 depicts the pattern of IMP on the P-face (Fig. 2*a*) and the E-face (Fig. 2*b*) of the PM of undiluted cells and on the P-face of the PM of cells fixed immediately after dilution to 0.86 M NaCl (Fig. 2*e*).

Control cells contained randomly distributed globular particles of 60–130 Å apparent diameter on the PM P-face. After

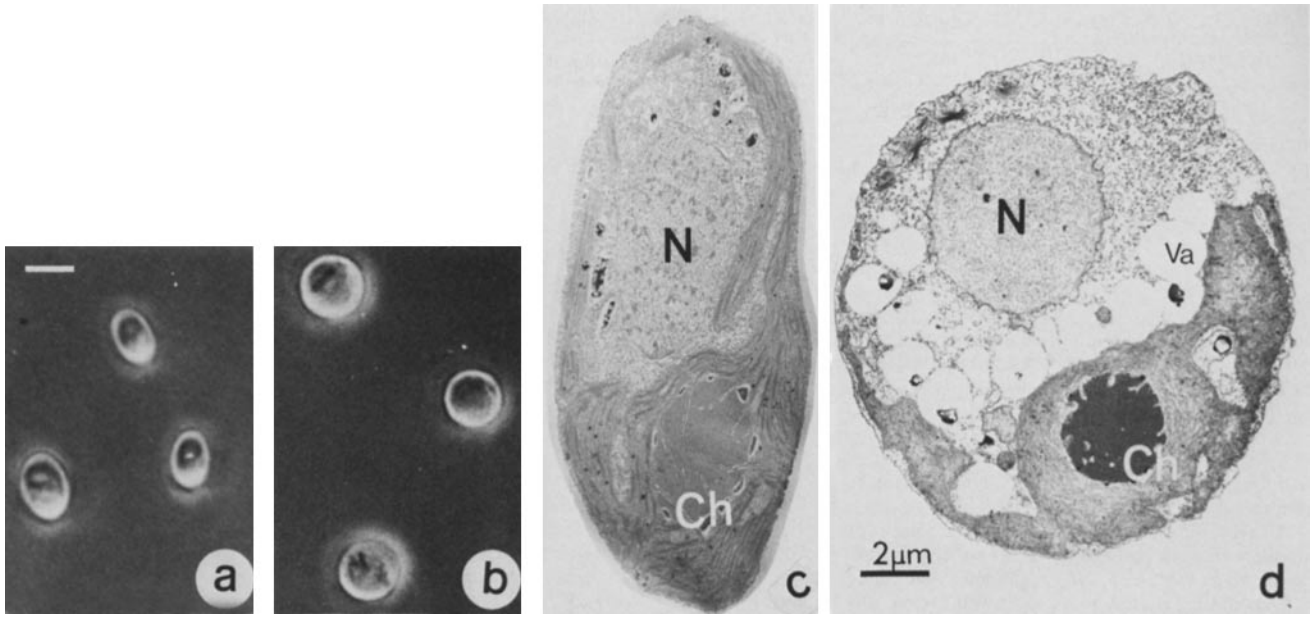

Figure 1. Dunaliella salina cell expansion caused by transferring cells from 1.71 M NaCl regular culture medium to 0.86 M NaCl medium as observed by light microscopy (*a* and *b*) and thin-section electron microscopy (*c* and *d*). (*a*) Light micrograph of control (undiluted) cells, showing their oval shape. Bar (for *a* and *b*), 10 μm. (*b*) 3 min after hypoosmotic shock, illustrating their spherical shape. (*c*) Thin-section electron micrograph of a control cell. *N*, nucleus; *Ch*, chloroplast. (*d*) Micrograph of a cell fixed 3 min after hypoosmotic shock. Vacuoles (*Va*) are more easily seen in the cytoplasm due to their expansion. Bar (for *c* and *d*), 2 μm.

Table II. Alterations in the Volume Occupied by the Major D. salina Cell Compartments after Hypoosmotic Shock

	Control culture ($n = 75$)		Diluted culture ($n = 71$)*		Volume (diluted)/ Volume (control)
	Volume μm^3/cell	Volume (% of total)	Volume (μm^3/cell)	Volume (% of total)	
Chloroplast	301.3	51.0	463.0	44.6	1.54
Nucleus	66.2	11.2	156.7	15.1	2.37
Vacuoles	27.8	4.7	99.6	9.6	3.58
Mitochondria	16.0	2.7	18.7‡	1.8	1.17
Golgi bodies	2.3	0.4	4.2§	0.4	1.83
Cytoplasm	173.7	29.4	288.6	27.8	1.66
Others¶	3.5	0.6	7.3¶	0.7	2.09
Total	590.8	100	1,038.1	100	

Mean volumes were determined by the morphometric procedures described in Materials and Methods. Except where noted, differences between values for diluted and control cultures were statistically significant at the 0.001 level.

* Cells were fixed for analysis 3 min after dilution from 1.71 to 0.86 M NaCl. *n* equals number of counted areas.

‡ $P < 0.2$.

§ $P < 0.4$.

¶ Lipid bodies and small numbers of unidentified organelles.

¶ $P < 0.1$.

Table III. Alterations in Surface Area Per Cell for Certain Organelles of D. salina Caused by Hypoosmotic Shock

	Surface area (μm^2/cell)	
Organelle	Control	Diluted*
Chloroplast	249.3	373.7
Nucleus	79.2	110.0
Mitochondria	87.4	131.8
Golgi bodies	43.7	17.6
ER	697.1	500.1

Morphometric analyses of surface area utilized a minimum of 19 separate measurements for each value. The mean surface area per cell for each organelle was calculated as described in Materials and Methods. All differences between control and diluted cells are statistically significant at the 0.001 level.

* Cells were fixed for analysis 3 min after dilution from 1.71 to 0.86 M NaCl.

dilution the PM P-face always showed concave depressions, most of which contained relatively few IMP. Depressed areas of this type were occasionally seen on the PM of undiluted control cells but were never observed in numbers approaching those shown in Figs. 2*e* and 3, *a* and *b*.

The P-face and the E-face of the PM fixed 3 min after dilution of the cells are shown in Fig. 3, *a* and *b*, respectively. Here again numerous roughly circular structures, some concave and some convex, were apparent. All contained a lower density of particles than was found in the surrounding PM. Replicas of the equivalent E-face of the PM from control cells rarely showed such structures. A similar pattern of circular structures in the PM of diluted cells but not control cells was observed in replicas of cells frozen without prior fixation.

During the initial rapid expansion after dilution, there was a decrease in the density of IMP (Table IV). Because of the wide variability encountered, most of the differences in particle density were not statistically highly significant according to the *t*-test (not assuming equal variance). Thus the changes must be considered only suggestive. However, based on the particle counts in Table IV and considering that the PM surface area actually increased by 53% (Table I), the total number of PM IMP per cell rose by 39% (P-face) and 27% (E-face). These additional particles were presumably introduced during fusion with vesicles of lower particle density (see below).

The small vesicles thought to be involved in fusion with

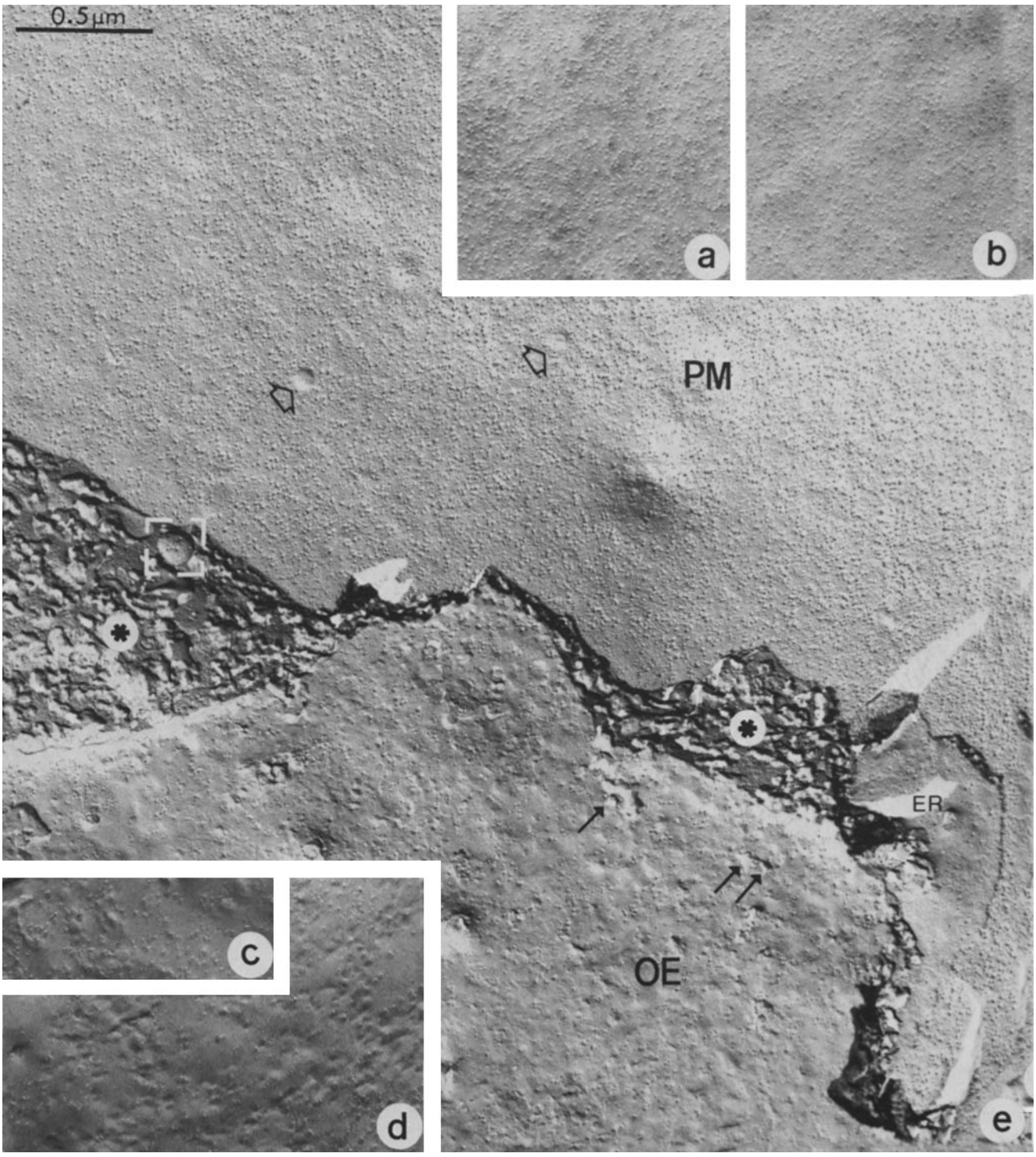

Figure 2. Plasma membrane and outer chloroplast envelope of control and hypoosmotically shocked *D. salina* as revealed by freeze-fracture electron microscopy. (*a*) P-face of control cell plasma membrane. (*b*) E-face of control cell plasma membrane. (*c*) P-face of control cell outer chloroplast envelope. (*d*) E-face of control cell outer chloroplast envelope. (*e*) Plasma membrane (*PM*) (P-face) and outer chloroplast envelope (*OE*) (E-face) immediately after hypoosmotic shock. Several concave dome-shaped structures are seen on the plasma membrane (arrow). Some of them have a reduced number of IMP. In the cytoplasm (*) cross-fractured between the plasma membrane and the outer chloroplast envelope, a vesicle ([]) and endoplasmic reticulum (*ER*) are seen. On the outer chloroplast envelope are seen irregularly margined fenestrations (arrows), which we interpret to be cross-fractures through protruding dome-shaped structures. Bar (for *a–e*), 0.5 µm.

the PM could also be detected in thin sections of the cells (Fig. 3*c*). The number of these vesicles present after dilution was much diminished. A close association of the small vesicles with the PM was sometimes observed, but continuity of membrane surface between vesicle and PM was not clearly distinguishable, perhaps due to the small size of the vesicles.

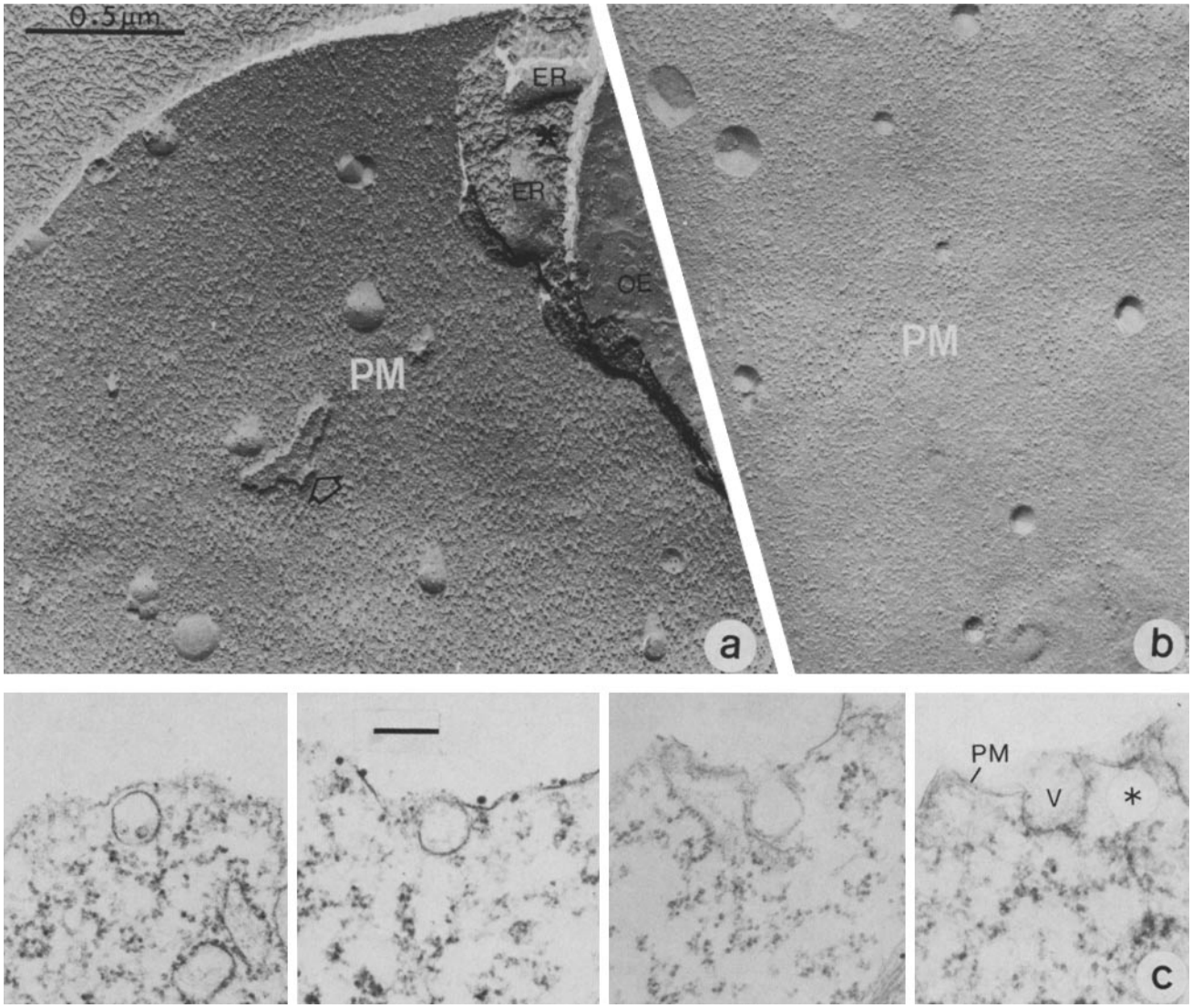

Figure 3. Plasma membrane alterations 3 min after hypoosmotic shock, as observed by freeze-fracture electron (*a* and *b*) and thin-section (*c*) electron microscopy. (*a*) E-face of plasma membrane (*PM*). Many dome-shaped structures are seen with fewer IMP than found on the PM. Endoplasmic reticula (*ER*) are seen in the cytoplasm (*) cross-fractured between the PM and outer chloroplast envelope (*OE*). Irregularly shaped membranous structure (arrow) may be an element of ER near the PM. Bar (for *a* and *b*), 0.5 μm. (*b*) P-face of plasma membrane (*PM*). Irregularly distributed concave dome-shaped structures are seen. (*c*) Relationship between plasma membrane (*PM*) and vesicles (*V*), as observed in a series of thin section electron micrographs. Sometimes small vesicles closely approach and appear to fuse with PM. *, cytoplasm. Bar, 0.2 μm.

Effects of Hypoosmotic Stress on the Chloroplast Envelope

The outer chloroplast envelope of control cells appeared in freeze-fracture replicas as an irregularly undulating membrane with a P-face (Fig. 2*c*) containing randomly distributed particles 70–120 Å in diameter at a density of 1,172 ± 434 particles/μm^2. The E-face was similar but with a lower particle density (893 ± 429/μm^2). The outer chloroplast envelope of cells fixed immediately after dilution was marked by more exaggerated depressions and irregular fenestrations (Figs. 2*e* and 4*a*).

By 3 min after diluting cells to 0.86 M NaCl, the outer chloroplast envelope exhibited numerous concave and convex structures sparsely populated with IMP (Fig. 4, *c*, *d*, and *e*). Particle counting was difficult here because of their occasionally aggregated state. Also, it was impossible to estimate accurately the overall surface area of the cup-shaped chloroplast before and after dilution, although morphometric analysis (see later) indicated a volume increase of 1.56× after dilution. There were irregular margined depressions of the P-face (Fig. 4, *a*, *d*, and *e*) and protrusions on the E-face (Fig. 4*c*), the latter being suggestive of the fracture plane following the elevated dome-shaped structures. This latter replica (Fig. 4*e*) illustrates that cells frozen without fixation and glycerol treatment have the same appearance as fixed cells. Micrographs of thin sections through chloroplasts of the diluted cells (Fig. 4*b*) revealed a close association, perhaps a fusion between small elements of the ER and the outer chloroplast envelope, perhaps accounting for the increased cross-fracturing in Fig. 4, *a*, *d*, and *e*.

Below the fracture plane of the chloroplast outer envelope and revealed in the bottom of the irregular depressions (Fig. 4*a*) were membranes that we believe to be fusing elements of

Table IV. Alterations of IMP Density in the PM and Outer Chloroplast Envelope after Hypoosmotic Shock

Membrane	Fracture face	Control cells	Time (after dilution) of cell fixation	
			0 min	3 min
PM	P-F	3,508 ± 548 (13)	3,125 ± 429 (12)*	3,311 ± 1,109 (27)
	E-F	2,085 ± 301 (10)	2,100 ± 355 (11)	1,729 ± 736 (24)*
OE	P-F	1,172 ± 434 (19)	1,458 ± 523 (36)‡	1,551 ± 617 (24)‡
	E-F	893 ± 429 (34)	978 ± 552 (16)	1,029 ± 524 (46)

Values are mean IMP/μm^2 ± SD. Numbers of areas counted are shown in parentheses. OE, outer chloroplast envelope.

* Difference from control value is statistically significant at the 0.1 level.

‡ Difference from control value is statistically significant at the 0.05 level.

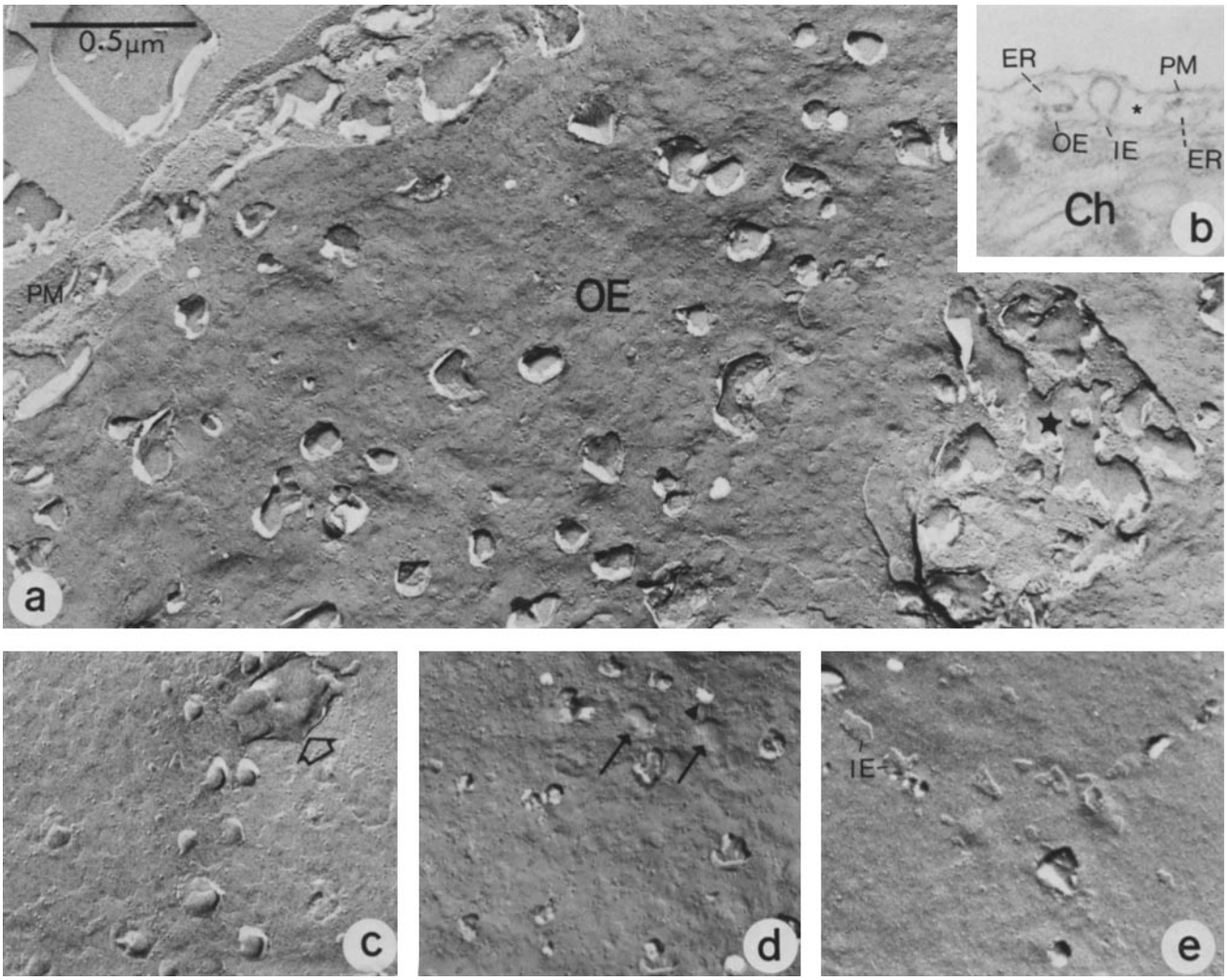

Figure 4. Membrane alterations of outer chloroplast envelope after hypoosmotic shock, as shown by freeze-fracture and thin-section electron microscopy. (*a*) P-face of outer chloroplast envelope (*OE*) immediately after hypoosmotic shock. Many depressed craters with irregular margins are randomly distributed. On the right side (*) there is a larger irregular depression around which IMP are relatively aggregated. (*b*) Thin section electron micrograph of cell treated as in Fig. 4*c*. The outer chloroplast envelope (*OE*) forms an elevated protrusion towards the cytoplasm (*), suggesting a fusion between OE and small elements of endoplasmic reticulum (*ER*) such as can be seen in the cytoplasm between PM and OE. (*c*) E-face of OE 3 min after hypoosmotic shock. Irregular protrusions are seen (arrow), but at the same time a few fenestrations are seen due to cross-fracturing through the protrusions (*d*). (*d*) P-face of OE 3 min after hypoosmotic shock. Irregular depressions are seen (arrow). (*e*) P-face of OE in cells quenched without fixation 3–5 min after hypoosmotic shock. These features are quite similar to that in Fig. 4*d*. Small areas of inner chloroplast envelope (*IE*) (E-face) are seen. Bar (for *a–e*), 0.5 μm.

the ER. These were also apparent in thin section micrographs of diluted cells (Fig. 4*b*) as small (40–120-nm diam) vesicles of ER appressed to or apparently fusing with the chloroplast outer envelope. In contrast, control cells contained numerous greatly elongated elements of ER that appeared upon occasion to be fused to the chloroplast outer envelope (Fig. 5).

By 3 min after dilution, the average surface area of ER per cell had declined to 72% of the value measured in control

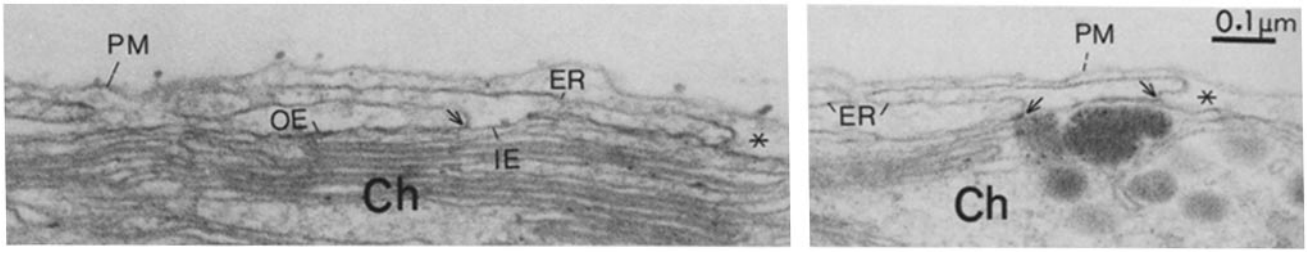

Figure 5. Thin section electron micrograph of control *Dunaliella* cells, showing many ER elements in the cytoplasm (*). One part of the ER is fused onto the outer chloroplast envelope (*OE*) (arrow). *IE*, inner chloroplast envelope; *Ch*, chloroplast; *PM*, plasma membrane. Bar, 0.1 μm.

Table V. Effect of Hypoosmotic Shock on Volume and Surface Area Per Cell of Vesicle Classes

Organelle	Volume (control)	Volume (diluted)	Volume (diluted) / Volume (control)	Surface area* (control)	Surface area* (diluted)	Surface area (diluted) / Surface area (control)
	μm^3	μm^3		μm^2	μm^2	
Vesicles (≤0.25 μm)	8.9	4.2	0.47	361.7	189.0	0.52
Vacuoles (>0.25 μm)	18.9	93.6	4.95	375.2	406.8‡	1.08

Mean organelle volumes and surface areas were calculated using the same procedures applied for Tables II and III, respectively. Cells that had been diluted from 1.71 to 0.86 M NaCl were fixed after 3 min. Except where noted, all differences between control and diluted cells were statistically significant at the 0.001 level.

* The surface area of vesicles and vacuoles includes the surface area of small vesicles or membranous structures seen inside of them.

‡ $P < 0.005$.

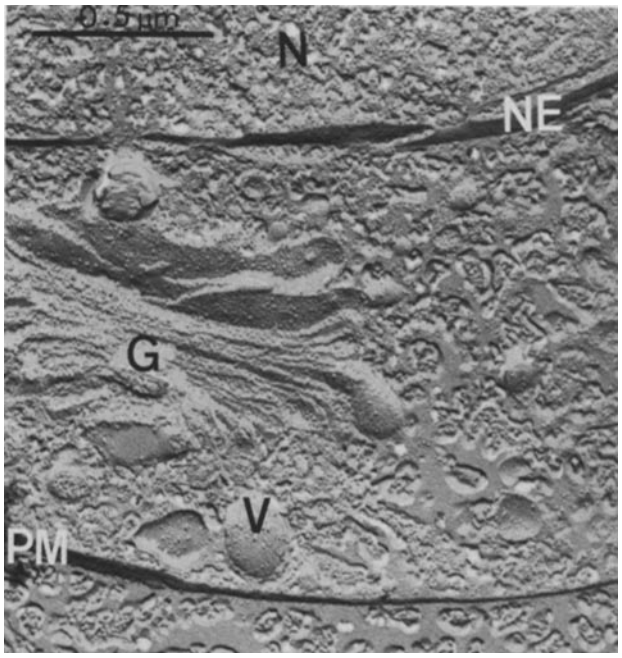

Figure 6. Freeze-fracture electron micrograph of small vesicles (*V*) in a cell 3 min after hypoosmotic shock. Small vesicles with a low density of IMP are seen near the Golgi body (*G*). These vesicles are quite similar in size to the dome-shaped structures seen on the plasma membrane (Fig. 3). *N*, nucleus; *NE*, nuclear envelope; *PM*, plasma membrane. Bar, 0.5 μm.

cells (Table III). Extensive ER membranes of the type illustrated in Fig. 5 were largely replaced by much smaller elements, still recognizable by having attached ribosomes. Considering the evidence presented above for membrane fusion with the outer chloroplast envelope, it is likely that ER serves as the reservoir of membrane material for chloroplast envelope expansion. The indications of an increased IMP density in expanded outer chloroplast envelope (Table IV) were to be expected after fusion of the outer chloroplast envelope with ER having a denser population of particles (P-face, 2,200 ± 428/μm^2; E-face, 1,310 ± 314/μm^2).

Few freeze-fracture replicas were found containing extensive fracture faces of the inner chloroplast envelope. Changes occurring in that membrane will not be considered at this time. No detectable structural alterations were noted in thylakoid membranes by freeze-fracture electron microscopy.

Effects of Hypoosmotic Stress on Other Organelles

Morphometric analysis (18, 20) of thin section electron micrographs (Table II) coupled with the absolute volume measurements of the whole cells shown in Table I permitted us to estimate the change in absolute volume of each major class of organelles. Some organelles changed very little after dilution. For example, mitochondria fixed 3 min after dilution to 0.86 M NaCl occupied a volume only 1.17× that measured in control cells. The largest volume increases were found in lipid bodies (2.09× volume of control), the nucleus (2.37× volume of control), and vacuoles (3.58× volume of control). The enlargement of vacuolar volume is readily apparent by comparing Fig. 1 *c* and 1 *d*. A similar morphometric analysis performed on cells fixed 60 min after dilution yielded volume measurements of the various organelles little different from those determined 3 min after dilution.

Vacuoles and vesicles were prominent in the cells. Morphometric analysis (Table V) of these structures in stressed and unstressed cells showed large volume changes per cell. Vacuoles were mainly localized in the anterior region of the cell and may constitute parts of a contractile vacuole system (10). The small vesicles, on the other hand, were more uniformly distributed through the cytoplasm, sometimes in association with the Golgi bodies (Fig. 6). The IMP density of these vesicles (P-face, 2,800 ± 738/μm^2; E-face, 1,087 ± 734/μm^2) was more than that of the dome-shaped structures found associated with the plasma membranes of diluted cells (Fig. 3, *a* and *b*) and was significantly lower than that of the PM itself. The bulk of our evidence (see below) suggests that the

small vesicles are the primary source of membrane for PM expansion.

Discussion

Our measurements confirm the observations of several other groups (e.g., 6, 9) that *Dunaliella* species can expand quickly and extensively to equalize an osmotic imbalance. In the present study dilution of the medium to half its normal salinity caused the cells to expand promptly to ~1.8× their original volume. Morphometric studies revealed that several types of intracellular organelles also expanded to nearly the same extent. Thus the chloroplast, which occupied 51% of the control cell volume, expanded to 1.54× its original size and the nucleus (11% of control cell volume) expanded 2.37×. These changes suggest that the glycerol and other osmotically active compounds made by *Dunaliella* to balance external NaCl (3) must be localized within at least some of the major intracellular compartments besides the cytoplasm, which itself enlarged in volume by a factor of 1.66 after dilution. Chemical evidence regarding sites of intracellular glycerol localization has not yet been obtained.

The rapid expansion of several membrane-bounded cell compartments creates a need for the addition of membrane material. Our studies have been focused on the growth of the PM and the chloroplast envelope. Evidence was obtained for the concerted fusion of many small vesicles with the PM. This fusion continued for at least 3 min, by which time the small vesicle population had become reduced by more than 50% (Table V). Evidence from electron microscopy leads us to conclude that the PM expansion relied mainly on small vesicles as a source of new membrane and did not normally involve fusion with elements of ER, despite the close proximity of these latter structures (Fig. 3*a*).

Expansion of the chloroplast envelope, in contrast, did seem to depend upon fusion with ER. The fusion process was more complex, perhaps because the pressure for expansion would come from the osmotically responsive inner chloroplast envelope forcing itself outward against the permeable outer envelope.

Chloroplast membrane expansion during normal growth is dependent to a considerable extent upon biosynthetic reactions taking place in the envelope, mainly the inner envelope membrane (see reference 7 for review). The inner envelope appears able in some higher plant species to provide additional membrane material that is detached as vesicles for migration to the growing thylakoids (22). On the other hand, the outer membrane is thought by many workers (reviewed in reference 7) to be derived not from the inner envelope but from extrachloroplastidal membranes such as the ER. It would be surprising if these normal sources of envelope structural lipids and proteins could supply the large amount of material needed during almost instantaneous expansion without being themselves noticeably depleted or distorted. There is ultrastructural evidence for a fusion of ER with the chloroplast outer envelope (4, 5), although direct fusion is not thought to be the major source of outer envelope components under normal growth conditions (21).

Based upon our observations of apparent fusion specificities during hypoosmotic stress, a balance sheet of intracellular membrane reorganization can be assembled. We postulate the co-existence of two semi-independent donor-acceptor systems supporting *Dunaliella* expansion under stress (Table VI). One system involves the increase of PM surface area at the expense of small vesicles. Certain vacuoles resemble the small vesicles structurally and may be interconvertible with them.

Table VI. Hypoosmotic Stress-induced Changes in Organelle Classes Thought to Interact by Fusion

	Increase*		Decrease*
PM	170.8	Vesicles	172.7
Vacuoles	31.6	Golgi	26.1
Subtotal	202.4	Subtotal	198.8
Chloroplasts	124.4	ER	197.0
Mitochondria	44.4		
Nuclei	30.8		
Subtotal	199.6	Subtotal	197.0
Total	402.0	Total	395.8

* Changes in μm^2, induced by dilution from 1.71 to 0.86 M NaCl for 3 min.

The ER may be the prime membrane donor in a separate interacting system supporting expansion of the chloroplast envelope and perhaps the mitochondrial and nuclear membranes. By tabulating these changes in membrane surface area that take place during the first 3 min after dilution (Table VI), a balance can be reached that is not incompatible with the proposed relationships.

At present no biochemical information is available to support the concept of organelle-selective fusion in *Dunaliella*. Although we have initiated a detailed study of *D. salina* membrane lipid composition (14, 15), it is still too early to know if certain membranes are enriched in fusogenic lipids. We found no indications in our freeze-fracture membrane replicas of hexagonal II phase lipids or lipidic particles (19).

Continued study of *Dunaliella* membrane structure and its possible modification under osmotic stress is needed to resolve a number of open questions regarding the physiology of these cells. For example, there is currently strong evidence both for (8) and against (2, 12) a significant leakage of glycerol from the cells grown in saline environments. Our preliminary findings (Yang, C. M., and G. A. Thompson, Jr.) show appreciable losses of *D. salina* intracellular glycerol to its growth medium, but it is not clear whether these losses occur through membrane permeability or via fusion of glycerol-containing intracellular vesicles with the PM.

Knowledge of the mechanisms utilized by *Dunaliella* for volume control may also be of value in understanding related phenomena in higher plants. Surprisingly, hyper- and hypoosmotic effects can pose a more serious threat to the survival of freezing plant tissue than does physical damage caused by ice crystals (17). Thawing rye protoplast preparations respond to the substantial dilution of their extracellular fluid by melting ice crystals through a vesicle fusion-assisted PM expansion similar in many respects to that which we have described above. We now plan to examine the effects of temperature variation on membrane fusion in *Dunaliella*.

The authors wish to express their gratitude to Dr. Raymond Legge for light microscopy of the cells (Fig. 1, *a* and *b*), to Mr. Y. Hozaki (Japan Highway Public Corporation) for assistance in calculating surface areas, to Dr. R. Mitchell for technical assistance with the electron microscope, and to Dr. James Mauseth for advice on morphometric analysis. We are indebted to the Cell Research Institute,

University of Texas, for the use of their electron microscopy facilities.

This work was supported in part by grants from the National Science foundation (PCM 8200289), the Robert A. Welch Foundation (F-350), and the National Cancer Institute (1 T32 CA09182).

Received for publication 8 March 1985, and in revised form 2 October 1985.

References

1. Avron, M., and A. Ben-Amotz. 1979. Metabolic adaptation of the alga *Dunaliella* to low water activity. *In* Strategies of Microbial Life in Extreme Environments. M. Shilo, editor. Verlag Chemie, Weinheim. 83–91.

2. Ben-Amotz, A., and M. Avron. 1973. The role of glycerol in the osmotic regulation of the halophilic alga *Dunaliella parva*. *Plant Physiol.* 51:875–878.

3. Brown, A. D., and L. J. Borowitzka. 1979. Halotolerance of *Dunaliella*. *In* Biochemistry and Physiology of Protozoa. Volume 1. 2nd ed. M. Levandowsky and S. H. Hutner, editors. Academic Press, Inc., New York. 139–190.

4. Cran, D. G., and A. F. Dyer. 1973. Membrane continuity and associations in the fern *Dryopteris borreri*. *Protoplasma*. 76:103–108.

5. Crotty, W. J., and M. C. Ledbetter. 1973. Membrane continuities involving chloroplasts and other organelles in plant cells. *Science (Wash. DC)*. 182:839–841.

6. Curtain, C. C., F. D. Looney, D. L. Regan, and N. M. Ivancic. 1983. Changes in the ordering of lipids in the membrane of *Dunaliella* in response to osmotic pressure changes. *Biochem. J.* 213:131–136.

7. Douce, R., M. A. Block, A.-J. Dorne, and J. Joyard. 1984. The plastid envelope membranes: their structure, composition, and role in chloroplast biogenesis. *In* Subcellular Biochemistry. Volume 10. D. B. Roodyn, editor. Plenum Publishing Corp., New York. 1–84.

8. Enhuber, G., and H. Gimmler. 1980. The glycerol permeability of the plasmalemma of the halotolerant green alga *Dunaliella parva* (Volvocales). *J. Phycol.* 16:524–532.

9. Gimmler, H., C. Wiedemann, and E. M. Moller. 1981. The metabolic response of the halotolerant green alga *Dunaliella parva* to hypertonic shocks. *Ber. Dtsch. Bot. Ges.* 94:613–634.

10. Guillard, R. R. L. 1960. A mutant of *Chlamydomonas moewusii* lacking contractile vacuoles. *J. Protozool.* 7:262–268.

11. Hoshaw, R. W., and L. Y. Maluf. 1981. Ultrastructure of the green flagellate *Dunaliella tertiolecta* (Chlorophyceae, Volvocales) with comparative notes on three other species. *Phycologia.* 20:199–206.

12. Lanyi, J. K., M. Avron, S. T. Bayley, T. D. Brock, A. D. Brown, P. S. Fitt, D. M. Griffin, N. H. Horowitz, D. J. Kushner, H. Larsen, B. Norkrans, H. G. Truper, and J. Weber. 1979. Life at low water activities. Group report. *In* Strategies of Microbial Life in Extreme Environments. M. Shilo, editor. Verlag Chemie, Weinheim. 125–135.

13. Lynch, D. V., and G. A. Thompson, Jr. 1982. Low temperature-induced alterations in the chloroplast and microsomal membranes of *Dunaliella salina*. *Plant Physiol.* 69:1369–1375.

14. Lynch, D. V., and G. A. Thompson, Jr. 1984. Microsomal phospholipid molecular species alterations during low temperature acclimation in *Dunaliella*. *Plant Physiol.* 74:193–197.

15. Lynch, D. V., and G. A. Thompson, Jr. 1984. Chloroplast phospholipid molecular species alterations during low temperature acclimation in *Dunaliella*. *Plant Physiol.* 74:198–203.

16. Spurr, A. J. 1969. A low viscosity epoxy-resin embedding medium for electron microscopy. *J. Ultrastruct. Res.* 26:31–43.

17. Steponkus, P. L. 1984. Role of the plasma membrane in freezing injury and cold acclimation. *Annu. Rev. Plant Physiol.* 35:543–584.

18. Toth, R. 1982. An introduction to morphometric cytology and its application to botanical research. *Am. J. Bot.* 69:1694–1706.

19. Verkleij, A. J. 1984. Lipidic intramembranous particles. *Biochim. Biophys. Acta.* 779:43–63.

20. Weibel, E. R. 1979. Stereological Methods. Vol. 1, Practical Methods for Biological Morphometry. Academic Press, Inc., New York. 415 pp.

21. Wellburn, A. R. 1982. Bioenergetic and ultrastructural changes associated with chloroplast development. *Int. Rev. Cytol.* 80:133–191.

22. Whatley, J. M., C. R. Hawes, J. C. Horne, and J. D. A. Kerr. 1982. The establishment of the plastid thylakoid system. *New Phytol.* 90:619–629.